Current Nanoscience, **2015,** *11,* **621-626**

HW-CVD Deposited Nanocrystalline Silicon Thin Films at Low Substrate Temperature with White-Blue Luminescence

A. Dutt[1], S. Godavarthi[2], Y. Matsumoto[1,*], G. Santana-Rodríguez[3], A. Avila[1], V. Sánchez[1] and G. Raina[4]

[1]*SEES, Electrical Engineering Department, Centro de Investigación y de Estudios Avanzados del IPN, Mexico City, 07360, Mexico;* [2]*Instituto de Ciencias Físicas, Universidad Nacional Autónoma de México, Avenida Universidad s/n, 62210 Cuernavaca, Morelos, México;* [3]*Instituto de Investigaciones en Materiales, Universidad Nacional Autónoma de México, Coyoacán 04510, Mexico;* [4]*Center for Nanotechnology Research, VIT University, Vellore, 632014, India*


Y. Matsumoto

Abstract: We report the influence of deposition pressure on the morphology and structural properties of the nanocrystalline silicon (nc-Si) particles embedded in amorphous silicon oxide (a-SiO_X) using hot wire chemical vapor deposition (HW-CVD). Catalyst material Tantalum (Ta) was employed for the decomposition of source gases in the reaction chamber. X-Ray diffraction (XRD) and Raman spectroscopy techniques were used to understand the thin film phase transition. Different bonds in the films, for example Si-H, were identified using Fourier transform infrared spectroscopy (FTIR) and the role of hydrogen species in inducing crystallization has been discussed. Particular pressure limit has been found to be adequate for the growth of silicon related crystalline particles. The samples deposited at substrate temperature of 200 °C, has shown photoluminescence spectra from blue to red zone, and the parts of the visible spectra has been found to be in correlation with the size of nc-Si and/or defects present in the thin film. This low temperature deposited Si based thin films using HW-CVD could be useful for a visible light emitting device production.

Keywords: Blue-white luminescence, deposition pressure, HW-CVD, hydrogen species, nc-Si, Si-H bonding.

1. INTRODUCTION

The relative abundance in nature and non-toxic property of Si as compared to other elements has made it a technologically important and widely researched material [1]. After the demonstration of photoluminescence properties of porous Si by Canham *et al.* [2], other groups started employing silicon towards optical devices. Since then, nc-Si has attracted much attention due to its benefits, for example their good photoluminescence response [3], possibility to tune the band gap [4] and reduced light-induced degradation [5].

To enhance the optical properties of silicon, the confinement effect plays a crucial role [6]. Embedding nc-Si in SiO_x is one of the ways to achieve quantum confinement due to the differences in the respective band gaps [7]. Previously many reports have been made with plasma enhanced chemical vapor deposition (PE-CVD) as the deposition technique, but more recently hot wire chemical vapor deposition (HW-CVD) has emerged as one of the well-known alternative deposition technique. HW-CVD has its own advantages like no plasma damage of thin films and more effective use of source gases [8, 9].

*Address correspondence to this author at the SEES, Electrical Engineering Department, Centro de Investigación y de Estudios Avanzados del IPN, Mexico City, 07360, Mexico; Tel: +52 57473800-3783;
E-mail: ymatsumo@cinvestav.mx

In this work, we report the synthesis of nc-Si crystallite particles embedded in a-SiO_x film using HW-CVD at low substrate temperature of 200 °C. The aim of this work was to understand the effect of the chamber pressure on photoluminescence properties of nc-Si embedded in SiOx by studying their morphological changes.

2. EXPERIMENTAL DETAILS

2.1. Sample Preparation

The HW-CVD system used for the depositions is a top-down type system, and has been described elsewhere [10, 11]. The distance between filament and substrate was kept constant at 5 cm. Two types of substrate materials were used i.e. Corning glass 2497C and boron doped crystalline silicon. The RCA method was used for cleaning the substrates [12]. The filament temperature (T_{fil}) and the substrate temperature (T_{subs}) were kept at 1750°C and 200°C, respectively. The flow rates of SiH_4, H_2, B_2H_6 and O_2 were maintained at 5, 5, 10 and 0.5 sccm respectively. After allowing the flow of all four gases, the pressure in the chamber was maintained at three different values: 0.082, 0.1 and 0.2 Torr (by controlling the valve), respectively. The growth rate of thin films was 1.92-2.01 Å/s at 0.1 Torr and for other two pressures, the deposition rate was lesser and the film thickness was in the order of 180 nm.

1875-6786/15 $58.00+.00

2.2. Characterization of Thin Films

In HW-CVD, the main nature of the deposited thin film depends on the radical formation from the source gases as they are introduced in the chamber, and when they react on the hot surface of the filament [13]. Resultant thin film properties and thus, also the optical response depends on number of variables such as filament temperature, substrate temperature, filament to substrate distance and the chamber pressure. In earlier work, the role of pressure (0.01 to 0.05 Torr) has been studied, finding that an increase in pressure results an increase in crystalline fraction too [14]. However, other authors reported the presence of an amorphous phase with an increase in pressure from 0.02 to 0.15 Torr [15]. Optical measurements as photoluminescence (PL) were never been observed previously with respect to crystallization of the film at low substrate temperatures. In these experiments, we found different phases for the three distinguishable pressure values (0.082, 0.1 and 0.2 Torr) and correlated the structural morphology with the observed PL spectra. Transitions among phases were analyzed by two techniques: X-Ray diffraction and Raman spectroscopy. XRD patterns were recoded with Siemens D5000. Raman spectra were taken using Jobin-Yvon T64000 spectrometer. Fourier Transform Infrared (FTIR) spectra were recorded in absorption mode with a resolution better than 1 cm^{-1}, within the 400 to 4000 cm^{-1} range, in a nitrogen atmosphere to identify the various bonds associated with thin films using nexus 470 Thermo Nicolet spectrometer. PL spectra were obtained using a Kimmon Koha He–Cd laser with excitation wavelength of 325 nm at room temperature.

3. RESULTS

Fig. (**1a**) shows the XRD pattern of the deposited thin films as a function of the deposition pressure. Phase transition from amorphous phase is observed with the increase in the chamber pressure. When the pressure is low (0.082 Torr), amorphous phase could be seen from the spectra, whereas, with the further increase in pressure to 0.1 Torr, respective planes (111), (220) and (311) related to Si could be seen. At 0.2 Torr, mixed phase nature of the thin film could be observed.

Raman spectra analysis is also one of the advanced characterization technique to characterize nc-Si thin films embedded in oxide matrix and especially to observe transition from amorphous to crystalline phases. For crystalline samples, the characteristic peak related to transverse optical vibrational mode of silicon appears at 520 cm^{-1}, whereas for amorphous phase can be found at 480 cm^{-1}. The phase transition can be observed by spotting the Raman peak position with respect to these two peaks [16].

Fig. (**1b**) shows the tendency of the Raman spectra of the films deposited at conditions mentioned in Fig (**1a**). Si peak position of the spectrum is observed at 480.09 cm^{-1} representing amorphous phase for the samples deposited at 0.082 Torr. However, when pressure is increased to 0.1 Torr, the peak position is shifted to 519 cm^{-1}. With further increase in pressure to 0.2 Torr, one broad shoulder at 485 cm^{-1} and an additional peak at 514 cm^{-1} can be observed.

FTIR spectroscopy results are shown in Fig. (**2**). From the spectra, Si-H wagging and stretching vibrational modes

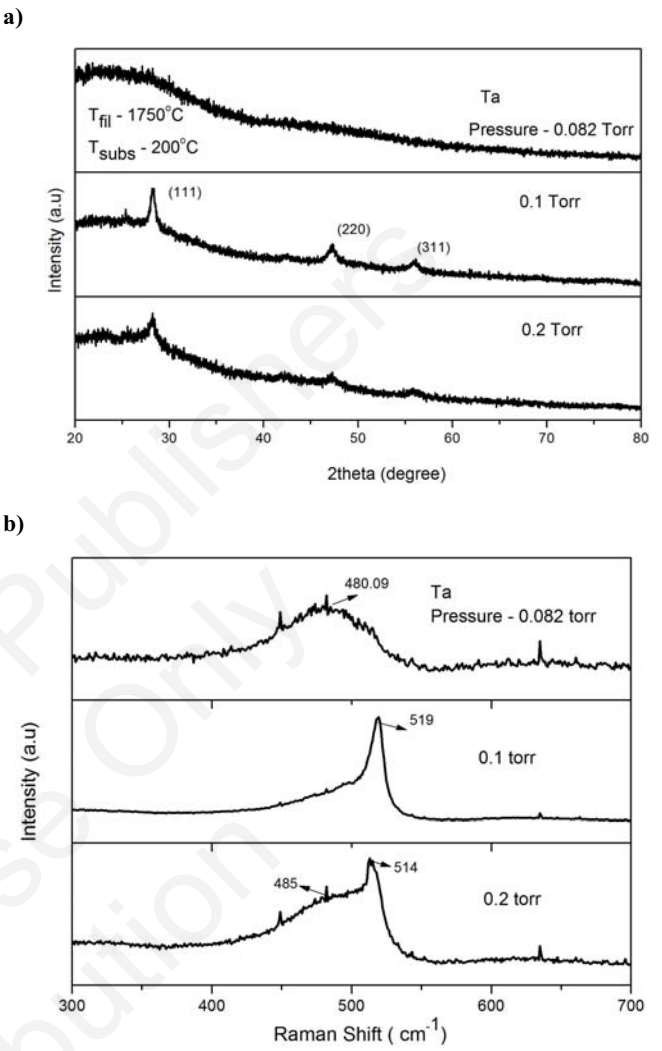

Fig. (1). (**a**) and (**b**), XRD and Raman spectra, respectively of films deposited with Ta wire, for several process pressures with T_{fil} = 1750°C, T_{subs} = 200°C and constant H_2/ SiH_4/B_2H_6/O_2 = 5/5/10/0.5 sccm flow.

can be observed at 640 cm^{-1} and 2000 cm^{-1}, respectively [17]. A double band centered at 2000 cm^{-1} and 2100 cm^{-1} could also be observed respectively. This double peak is evolved with the change in the pressure value. The same observations have been made by other groups and are related with the variation in hydrogen concentration in the thin films [14, 18]. According to the reported work, the peak at 2100 cm^{-1} corresponds to the stretching vibration mode of dihydride species Si-H_2 [19, 20]. In our experiments, no other significant shift in the peaks has been observed only apart that for crystalline sample movement in bonding state from 2000 cm^{-1} to 2100 cm^{-1} has been observed. On the other hand for amorphous samples broad peak could be observed at 2000 cm^{-1}.

Fig. (**3**) illustrates the comparison of (PL) spectra from Ta deposited samples at different pressure values. In the case of 0.082 Torr, one broad shoulder is observed between near 500 nm and 550 nm. With the increase in pressure to 0.1 Torr, the peak position shifted to near 480 nm and one

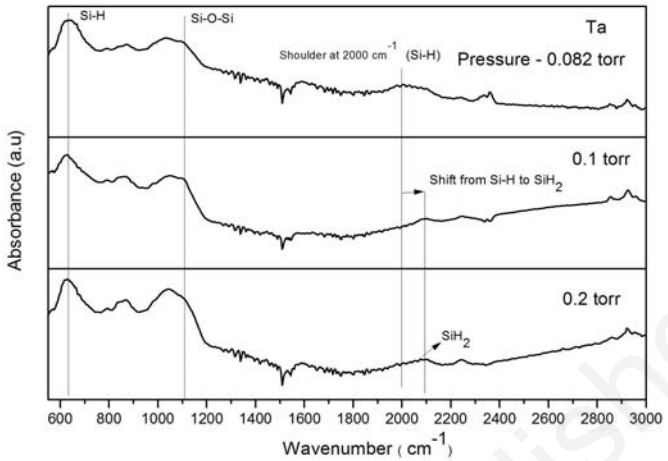

Fig. (2). FTIR spectra of nc-Si/SiO_2 film deposited using HW-CVD at various process pressures.

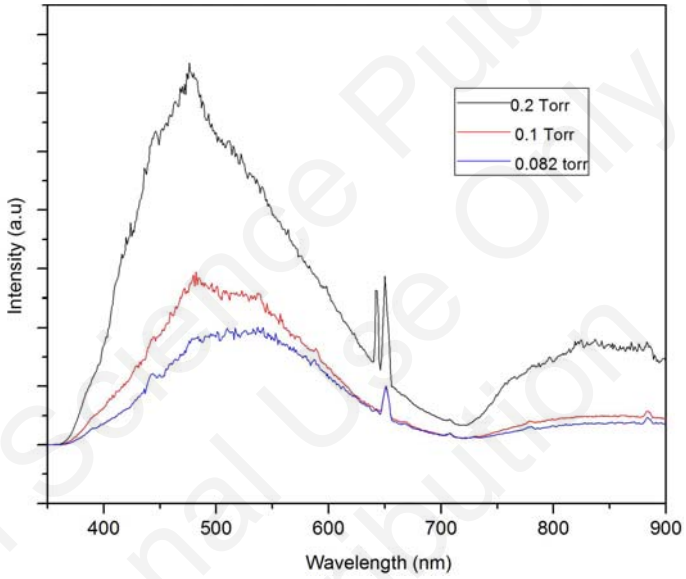

Fig. (3). PL spectra of films deposited with Ta filament at pressures of 0.082, 0.1 and 0.2 Torr.

more shoulder could be observed at around 530 nm. With further increase in pressure to 0.2 Torr, peak at 480 nm becomes more intense and bright blue-white luminescence emission was observed. However, the possible PL mechanism could be due to the electron-hole recombination at nc-Si/SiOx interface from particles observed in HRTEM image (Fig. **4**) [21, 22] or it could be due to defect sites like non-bridging oxygen hole center (NBOHC) [23]. More analysis regarding the emission mechanism has been given in following section.

4. DISCUSSIONS

In HW-CVD, as the foremost gas molecules are introduced into the chamber with the course of time and various reaction phases they get converted into different radical spe-

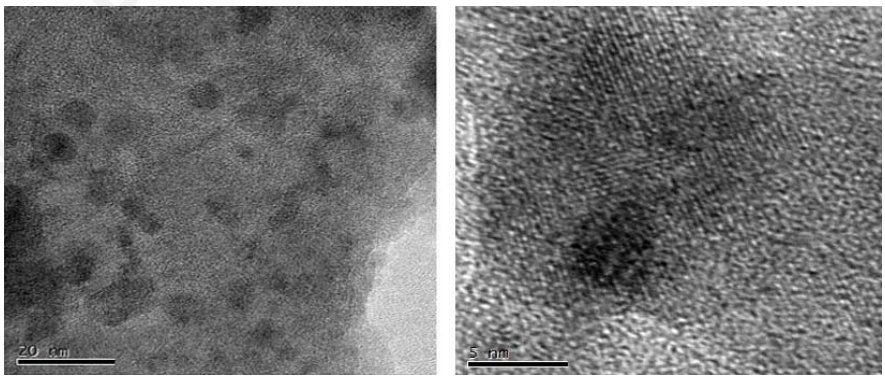

Fig. (4). HRTEM images showing the small nanoparticles of various size distributions at 0.1 and 0.2 Torr.

cies. The reaction among various primary radicals subsequently generates the secondary radicals [13] which finally influences the thin film properties. Formation of secondary radical species like SiH_x ($1 \leq x \leq 4$) depends on number of factors, for example the hydrogen concentration, chamber pressure and distance from filament to substrate [14]. When the pressure is less (0.082 Torr), an amorphous phase is detected using both Raman and XRD. FTIR absorption broad band is observed at 2000 cm^{-1} i.e. representing Si-H bonding. At relatively higher pressure i.e. 0.1 Torr; crystalline phase is identified by XRD and Raman. As a result, peak shift in the absorbance band from 2000 cm^{-1} to 2100 cm^{-1} [24, 25] is observed [26]. This specific peak shift shows the importance of the $Si\text{-}H_2$ species for developing the crystalline phases [20, 26, 27]. The role of $Si\text{-}H_2$ radicals on crystallization is verified by performing another set of experiments with increasing the filament temperature (T_{fil}) and the results are shown in Fig. (**5a** and **b**). From the respective figures, transition from amorphous to crystalline phase and correspondingly from Si-H to $Si\text{-}H_2$ bonding is observed at 1700 °C, which authenticates the role of $Si\text{-}H_2$ in inducing crystallization.

With further increase in pressure up to 0.2 Torr, a mixed phase is detected for the film. By the increase in deposition pressure after a certain limit, it results an increase in radical density, which reduces the mean free path of the radicals [18]. This consequence in proliferation of the number of collisions, which may reduce the essential radicals reaching the substrate required for the crystallization [28].

Fig. (**4**) shows the HRTEM image of Si nanocrystallites embedded in silicon oxide thin films deposited at 0.1 and 0.2 Torr. Shift in the visible spectra of PL for 0.1 and 0.2 Torr in Fig. (**3**) can be explained using the concept of quantum confinement effect. The PL peak position shifted to lower wavelength with the decrease in the grain size for 0.2 Torr and even the intensity is much more as compared to the PL spectra for 0.1 Torr. The PL spectra observed for 0.082 Torr could be correlated to Si-H bonding present [29] or it could be likewise related to surface trapped exciton states [30]. In one of the recent reports, UV emission from silicon thin films has been correlated with the non-bridging oxygen hole centers (NBOHCs) and Si-OH surface complexes [31],

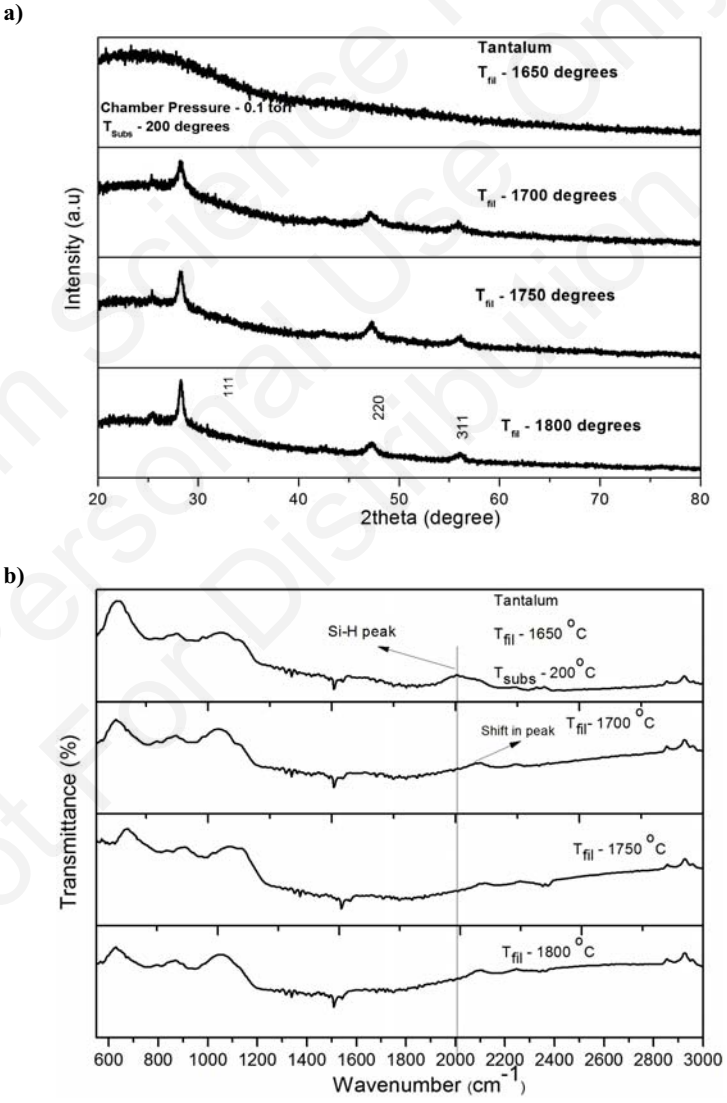

Fig. (5). (**a**) and (**b**), XRD and FTIR spectra, respectively of samples deposited with Ta wire at different filament temperatures (Tfil), with H_2/ $SiH_4/B_2H_6/O_2$ = 5/5/10/0.5 sccm flow at 0.1 Torr.

whereas other report have illustrated confinement as the cause of visible emission [32]. In other work, authors showed that some part of the visible emission spectra arises from the respective defect states and other as an outcome of confinement effect [33]. In the present case, kind of blue shift observed (0.1 and 0.2 Torr) for the intense visible emission strongly remarks the role of confinement in inducing the energy level traps for the particular emission.

5. CONCLUSION

Influence of the deposition pressure on the phase-transition of nanocrystalline silicon thin films developed using HW-CVD was studied. Using XRD, Raman, HRTEM and FTIR, changes in the morphological and optical properties in the films were made. In general, thin films demonstrated in the present work exhibited blue-white luminescence from as deposited samples without any post heat treatment processes. PL emission for the films deposited at 0.1 and 0.2 Torr was explained with the quantum confinement effect, whereas for the film deposited at 0.082 Torr it can be explained with the defect states. Room temperature observed intense visible emission in this work shows the importance of this technique to be used for future optoelectronic device applications.

CONFLICT OF INTEREST

The authors confirm that this article content has no conflict of interest.

ACKNOWLEDGEMENTS

The authors thank Angela Gabriela López for sample preparations. The authors are indebted to Marcela Guerrero, Alejandra García and Dr. Jaime Santoyo of Physics Department for XRD, Raman and TEM measurements, respectively. Also, the authors are thankful to Adolfo Tavira Fuentes for his contribution in measuring photoluminescence spectra. This project is supported by the National Council of Science and Technology (CONACyT) N° CB2009 -128723 also by the Institute of Science and Technology of Federal District (ICyT 326/11).

REFERENCES

[1] Palanna, O.G. *Engineering Chemistry*, Tata Mcgraw Hill Education Pvt. Ltd.: India, **2009**.

[2] Canham, L.T. Silicon quantum wire array fabrication by electrochemical and chemical dissolution of wafers. *Appl. Phys. Lett*., **1990**, *57* , 1046-1048.

[3] Takagi, H.; Ogawa, H,; Yamazabi, Y.; Ishizaki, A. ; Nakakiri, T. Quantum size effects on photoluminescence in ultrafine Si particles. *Appl. Phys. Lett*., **1990**, *56*, 2379-2380.

[4] Kitao, J.; Harada, H.; Yoshida, N.; Kasuya, Y.; Nishio, M.; Sakamoto, T.; Itoh, T.; Nonomura, S. Absorption coefficient spectra of μc-Si in the low-energy region 0.4–1.2 eV. *Sol. Energy Mater Sol. Cells*, **2001**, *66*, 245-251.

[5] Shah, A.V.; Meier, J.; Vallat-Sauvain, E.; Wyrsch, N.; Kroll, U.; Droz, C.; Graf, U. Material and solar cell research in microcrystalline silicon. *Sol. Energy Mater. Sol. Cells*, **2003**, *78*, 469-491.

[6] Koch, F.; Petrova-Koch, V.; Muschik, T. The luminescence of porous Si: the case for the surface state mechanism. *J. Luminesc*, **1993**, *57*, 271-281.

[7] Wolkin, M.V.; Jorne, J.; Fauchet, P.M.; Allan, G. ; Delerue, C. Electronic states and luminescence in porous silicon quantum dots: the role of oxygen. *Phys. Rev. Lett*., **1999**, *82*, 197-200.

[8] Matsumura, H. Catalytic Chemical Vapor Deposition (CTC–CVD) Method Producing High Quality Hydrogenated Amorphous Silicon. *Jpn. J. Appl. Phys*, **1986**, *25*, 949-951.

[9] Mahan, A.H.; Carapella, J.; Crandall, R.S.; Balberg, I. Deposition of Device Quality, Low H Content Amorphous Silicon. *J. Appl. Phys*., **1991**, *69*, 6728-6730.

[10] Matsumoto, Y. Hot wire-CVD deposited a-SiOx and its characterization. *Thin Solid Films*, **2006**, *501*, 95-97.

[11] Matsumoto, Y.; Godavarthi, S.; Ortega, M.; Sánchez, V.; Velumani, S.; Mallick, P.S. Size modulation of nanocrystalline silicon embedded in amorphous silicon oxide by Cat-CVD. *Thin Solid Films*, **2011**, *519*, 4498-4501.

[12] Kern, W.; Puotinen, D.A. Cleaning solutions based on hydrogen peroxide for use in silicon semiconductor technology. *RCA Rev*, **1970**, *31*, 187-206.

[13] Nakamura, S.; Matsumoto, K.; Susa, A.; Koshi, M. Reaction mechanism of silicon Cat-CVD. *J. Non-Cryst. Solids*, **2006**, *352*, 919-924.

[14] Bakr, N.A.; Funde, A.M.; Wamana, V.S.; Kamble, M.M.; Hawaldar, R.R.; Amalnerkar, V.G.Sathe, D.P.; Gosavi, S.W.; Jadkar, S.R. Influence of deposition pressure on structural, optical and electrical properties of nc-Si: H films deposited by HW-CVD. *J. Phys. Chem. Solids*, **2011**, *72*, 685-691.

[15] Klein, S.; Finger, F.; Carius, R.; Stutzmann, M. Deposition of microcrystalline silicon prepared by hot-wire chemical-vapor deposition: The influence of the deposition parameters on the material properties and solar cell performance. *J. Appl. Phys*., **2005**, *98*, 024905- 024918.

[16] Viera, G.; Huet, S.; Boufendi, L. Crystal size and temperature measurements in nanostructured silicon using Raman spectroscopy. *J. Appl. Phys*., **2001**, *90*, 4175-4183.

[17] Lucovsky, G.; Nemanich, R.J.; Knights, J.C. Structural interpretation of the vibrational patterns of a-Si: H alloys. *Phys. Rev. B*, **1979**, *19*, 2064-2073.

[18] Jadkar, S.R.; Sali, J.V.; Kshirsagar, S.T.; Takwale, M.G. Influence of process pressure on HW-CVD deposited a-Si:H thin films. *Sol. Energy Mater. Sol. Cells*., **2005**, *85*, 301-312.

[19] Tsu, D.V.; Lucovsky, G.; Dadison, B.N. Effect of the neighbors and alloy matrix on SiH stretching vibrations in the amorphous SiOr: H (0<r<2) alloy system. *Phys. Rev. B*., **1989**, *40*, 1795-1805.

[20] Veprek, S.; Veprek-Heijman, Maritza G.J. Possible contribution of SiH_2 and SiH_3 in the plasma-induced deposition of amorphous silicon from silane. *Appl. Phys. Lett*., **1990**, *56*, 1766-1768.

[21] Kenyon, A.J.; Trwoga, P.F.; Pitt, C.W.; Rehm, G. J. The origin of photoluminescence from thin films of silicon rich silica. *J. Appl. Phys*., **1996**, *79*, 9291-9300.

[22] Shimizu-Iwayama, T.; Fujita, K.; Nakao, S.; Saitoh, K.; Fujita, T.; Itoh, N. Visible photoluminescence in Si+- implanted silica glass. *J. Appl. Phys*., **1994**, *75*, 7779-7783.

[23] Skuja, L. Optically Active Oxygen-Deficiency-Related Centers in Amorphous Silicon Dioxide. *J. Non-Cryst. Solids*, **1998**, *239*, 16-48.

[24] Knights, J.C.; Lucovsky, G.; Nemanich, R.J. Defects in Plasma-deposited a-Si:H. *J. Non-Cryst. Solids*, **1979**, *32*, 393-403.

[25] Han, D.; Wang, K.; Owens, J.M.; Gedvilas, L.; Nelson, B.; Habuchi, H.; Tanaka, M. Hydrogen Structures and the Optoelectronic Properties in Transition Films from Amorphous to Microcrystalline Silicon Prepared by Hot-Wire Chemical Vapor Deposition. *J. Appl. Phys.*, **2003**, *93*, 3776- 3783.

[26] Itoh, T.; Yamamoto, K.; Ushikoshi, K.; Nonomura, S.; Nitta S. Characterization and role of hydrogen in nc-Si: H. *J. Non-Cryst. Solids*, **2000**, *266-269*, 201-205.

[27] Veprek, S. Controversies in the suggested mechanisms of plasma-induced deposition of silicon from silane. *Thin Solid Films*, **1989**, *175*, 129-139.

[28] Otobe, M.; Oda, S. The role of hydrogen radicals in nucleation and growth of nanocrystalline silicon. *J. Non-Cryst. Solids*, **1993**, *164-166*, 993-996.

[29] Glinka, Y.D., Lin, S.H.; Chen, Y.T. The photoluminescence from hydrogen-related species in composites of SiO_2 nanoparticles. *Appl. Phys. Lett.,* **1999**, *75*, 778 -780.

[30] Itoh, C.; Tanimura, K.; Itoh, N. Optical studies of self-trapped excitons in SiO_2. *J. Phys. C*, **1988**, *21*, 4693-4702.

[31] Liang, C.D.; Hsiung, H.M.; Lay, G.T; Jiann, S.; Ming, C.B.; Chi, L.S.; Chun, C.H. Eliminated UV Light Emitted from Nanostruc-

tured Silica Thin Film using H2 Plasma by ICP-CVD. *Curr. Nanosci*, **2011**, *7*, 240-244.

[32] Goni, A.R.; Muniz, L.R.; Reparaz, J.S.; Alonso, M.I.; Arbiol, J.; Garriga, M.; Rurali, R. Using high pressure to unravel the mechanism of visible emission in amorphous Si/SiOx nanoparticles. *Phys. Rev. B*., **2014**, *89*, 045428-13.

[33] Spallino, L.; Vaccaro, L.; Sciortino, L.; Agnello, S.; Buscarino, G.; Cannas, M.; Gelardi, F. M. Visible-ultraviolet vibronic emission of silica nanoparticles. *Phys. Chem. Chem. Phys*., **2014**, *16*, 22028-22034.

Received: October 26, 2014 Revised: February 06, 2015 Accepted: February 21, 2015